Single-molecule imaging of DNAs with sticky ends at water/fused silica interface

by

Slavica Isailovic

A thesis submitted to the graduate faculty
in partial fulfillment of the requirements for the degree of
MASTER OF SCIENCE

Major: Analytical Chemistry

Program of Study Committee:
Edward S. Yeung, Major Professor
Patricia A. Thiel
Gordon J. Miller

Iowa State University
Ames, Iowa
2005

Graduate College

Iowa State University

This is to certify that the master's thesis of

Slavica Isailovic

has met the thesis requirements of Iowa State University

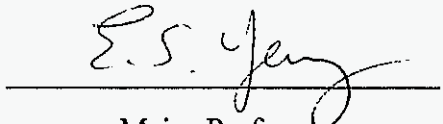

Major Professor

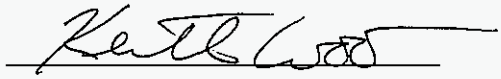

For the Major Program

TABLE OF CONTENTS

ABSTRACT

Total internal reflection fluorescence microscopy (TIRFM) was used to study intermolecular interactions of DNAs with unpaired (sticky) ends of different lengths at water/fused silica interface at the single-molecule level. Evanescent field residence time, linear velocity and adsorption/desorption frequency were measured in a microchannel for individual DNA molecules from T7, Lambda, and PSP3 phages at various pH values. The longest residence times and the highest adsorption/desorption frequencies at the constant flow at pH 5.5 were found for PSP3 DNA, followed by lower values for Lambda DNA, and the lowest values for T7 DNA. Since T7, Lambda, and PSP3 DNA molecules contain none, twelve and nineteen unpaired bases, respectively, it was concluded that the affinity of DNAs for the surface increases with the length of the sticky ends. This confirms that hydrophobic and hydrogen-bonding interactions between sticky ends and fused-silica surface are driving forces for DNA adsorption at the fused-silica surface. Described single-molecule methodology and results therein can be valuable for investigation of interactions in liquid chromatography, as well as for design of DNA hybridization sensors and drug delivery systems.

CHAPTER 1. INTRODUCTION

Single molecule studies

The advances in sensitive instrumentation in last decades have allowed for the detection, identification, and dynamic studies of single molecules. This measurement capability provided new tools to address important problems and to explore new frontiers in many scientific disciplines, such as chemistry, physics, biology, molecular biology, molecular medicine and nanomaterials.[1-17]

Single molecule approach has the advantage of removing ensemble average from measurement and direct observation of dynamical changes without need for synchronization. Standard ensemble measurements give the average value of a parameter for a large number of (presumably identical) copies of the system of interest. In contrast, single-molecule measurements completely remove the ensemble averaging and the results come from many single molecules, one by one. This allows construction of a frequency histogram of the actual distribution of values for an experimental parameter, rather than just the average (mean) value of the distribution. The distribution contains more information than the average value alone. The shape of the full distribution can be examined to see whether there are multiple peaks, or whether it has a strongly skewed shape. These details of the distribution become important when the system under study is inhomogeneous, which is often the case for many complex condensed matter environments. A single molecule can be viewed as a local reporter of its environment and local fields in its immediate vicinity. Heterogeneity of bio-molecules comes, for example, from different folded states or different configurations the various individual copies of a protein or DNA can have.

Another reason for performing experiments in the single-molecule regime is that they remove the need for synchronization of many single molecules undergoing a time-dependent process. For example, an enzymatic system can be in one of several catalytic states. For the ensemble measurements, synchronization is required, whereas if individuals are observed, any one

member of the ensemble is in only one state at a given time, and thus the specific sequence of binding, hydrolysis, and other catalytic steps is available for study.

Single-molecule techniques also have the possibility of observing new effects in unexplored regimes. For example, some single-molecule systems have unexpectedly shown some form of fluctuating, flickering, or stochastic behavior as result of a change in their local environment or thermally- and photo-induced changes of molecular conformations and orientations.

Several successful lines of research on individual species include the spectroscopy of single electrons or ions confined in electromagnetic traps,[18-20] scanning tunneling microscopy and atomic force microscopy of atoms and molecules on surfaces,[21-24] the study of ion currents in single transmembrane channels,[25] force measurements on single molecular motors using optical traps,[26-27] and optical single molecule spectroscopy (SMS) of molecules in condensed phase.[28-31] Due to their previously mentioned advantages in studying heterogeneous and complex systems, single molecule techniques have gained increasing attention in the field of life science.[32] Relative simplicity and noninvasive nature of optical single bio-molecule spectroscopy in room-temperature liquids and on surfaces makes SMS often a method of choice in biologically relevant studies of molecular interactions, molecular motions, and chemical kinetics.

Principles of Optical Single Molecule Spectroscopy

In order to use optical radiation to probe a single molecule on a surface, in a liquid, or inside a solid sample two requirements have to be met: only the molecule of interest is in resonance in the volume probed by the laser, and signal-to-noise ratio (SNR) for the single molecule signal is greater than unity for a reasonable averaging time.

At room temperature, guaranteeing that only one molecule is in resonance is generally achieved by a combination of focusing the laser to a small probe volume ($1 - 100\ \mu m^3$, even down to $10^{-4}\ \mu m^3$ for near-field methods), using an ultrapure host matrix, and selecting an

ultralow concentration of the molecule of interest.

Achieving the required SNR requires maximizing signal while minimizing backgrounds. To obtain as large a signal as possible, a combination of small focal volume, large absorption cross section, high photostability, weak bottlenecks into dark states such as triplet states, and operation below saturation of the molecular absorption is employed.

The low background and high signal-to-noise are the reasons laser-induced *fluorescence* has become the most widely used optical method. Fluorescence is the result of three-stage process that occurs in certain molecules (generally polyaromatic hydrocarbons or heterocycles) called fluorophores or fluorescent dyes. The process responsible for the florescence of fluorescent molecules is illustrated by the simple electronic-state diagram (Jablonski diagram) shown in Figure 1.1. A photon of energy $h\nu_{EX}$ is supplied by an external source such as an incandescent lamp or a laser and absorbed by the fluorophore, creating an excited electronic singlet state (S_1'). The excited state exists for a finite time (typically 1–10 nanoseconds). During this time, the fluorophore undergoes conformational changes and is also subject to a multitude of possible interactions with its molecular environment. These processes have two important consequences. First, the energy of S_1' is partially dissipated, yielding a relaxed singlet excited state (S_1) from which fluorescence emission originates. Second, not all the molecules initially excited by absorption return to the ground state (S_0) by fluorescence emission. Other processes such as collisional quenching, fluorescence resonance energy transfer (FRET) and intersystem crossing may also depopulate S_1. The fluorescence quantum yield, which is the ratio of the number of fluorescence photons emitted to the number of photons absorbed, is a measure of the relative extent to which these processes occur. A photon of energy $h\nu_{EM}$ is emitted, returning the fluorophore to its ground state S_0. Due to energy dissipation during the excited-state lifetime, the energy of this photon is lower, and therefore of longer wavelength, than the excitation photon $h\nu_{EX}$. This difference in energy or wavelength is called the Stokes shift. The Stokes shift is fundamental to the sensitivity of fluorescence techniques because it allows emission photons to be detected against a low background, isolated from excitation photons. In contrast, absorption

spectrophotometry requires measurement of transmitted light relative to high incident light levels at the same wavelength. The entire fluorescence process is cyclical. Unless the fluorophore is irreversibly destroyed in the excited state (photobleached), the same fluorophore can be repeatedly excited and detected (10^5-10^6 times). The fact that a single fluorophore can generate many thousands of detectable photons is fundamental to the high sensitivity of fluorescence detection techniques.

The key challenge in fluorescence single molecule detection is to reduce the background interference, which may arise from Raman scattering, Rayleigh scattering, and impurity fluorescence of the bulk medium containing the molecule of interest. In addition to use of ultrapure solvents as mentioned before, background interference can be suppressed by the use of high-performance optical filters, gated detectors in combination with pulsed lasers, and the reduction of illuminated-sample volume through the use of laser excitation in the confocal, near-field, and evanescent field configurations. These special excitation geometries direct the laser beam to probe a small volume or a thin sample layer.

Optical Single Molecule Spectroscopy Techniques

A number of optical methods have been developed to study single molecules. They differ in sampling conditions and means of delivering excitation energy, but all of them share the need to isolate single molecules for detection. The most useful approach is to isolate molecules on a surface or in dilute solution, i.e. individual molecules are spatially separated from each other in the area or volume probed by a laser beam.

The methods for detecting and identifying single molecules in *liquid streams* are based either on hydrodynamic focusing or tight laser beam focusing. In either case, picoliter volumes are interrogated and single molecules are identified as bursts of fluorescence photons in very dilute solutions. Fluorescence signals are collected at 90 degrees with respect to the direction of the laser beam before passing through spatial and spectral filters to the detection system.

The main concepts of *microdroplets* is to confine a single molecule in a picoliter-sized droplet and to use an electrodynamic trap for levitating the droplet so that the molecule can be interrogated by a laser beam for an extended period of time.

Near-field scanning optical microscopy (NSOM) is a technique with sub-diffraction spatial resolution. The resolution is only limited by the size of the aperture of the probe tip, which is often a pulled micropipette or a tapered single-mode fiber. The excitation light diverges rapidly after near-field region providing efficient background rejection (due to small illumination volume). High photon flux is delivered by the tapered single-mode fiber and single molecules are excited by a strong evanescent wave near the tip. The benefits of near-field microscopy are its improved spatial resolution and the ability to correlate spectroscopic information with topographic data. However, low power throughput, poor reproducibility in tip preparation, and sample perturbation by the coated fiber probe are the main disadvantages of this technique.

In *confocal microscopy*, a laser beam is brought to its diffraction-limited focus inside a sample using an oil-immersion, high-numerical–aperture objective. A small pinhole is placed at the image plane to reject light from out-of-focus regions. This arrangement defines a small femtoliter volume in the sample for which probability of finding two molecules is very small for nano- and pico-molar solutions. Although its resolution is diffraction-limited, the confocal approach has several important advantages: It provides an unlimited laser throughput, a three-dimensional sectioning capability, and noninvasive detection. These features, together with high sensitivity and experimental simplicity, make confocal fluorescence detection a powerful method. Because a confocal laser beam probes a single point at a time, scanning is required to survey a large area of interest. This method is well suited for single-point spectroscopy and kinetic monitoring (on the millisecond timescale) but it is intrinsically time-consuming if a large area needs to be examined.

Evanescent wave excitation is normally achieved by total internal reflection at the glass-liquid/air interface. Total internal reflection is a phenomenon that happens when light traveling from medium of higher index of refraction n_1 (glass, quartz) to medium of lower

index of refraction n_2 (air or water) completely reflects from the interface (Figure 1.2). This happens if the angle of incidence equals or exceeds the critical angle θ_c, defined by $\theta_c = \sin^{-1}(n_2/n_1)$. The intensity of evanescent field I (z) at distance z from the interface is given as $I(z)=I_o e^{-z/d}$, where I_o is light intensity at the interface (z = 0) and d is penetration depth of evanescent field. At the interface the optical electromagnetic field does not abruptly drop to zero but decays exponentially into the liquid phase (or air). Penetration depth is defined as $d = \lambda/4\pi[n_1^2\sin^2\theta - n_2^2]^{-1/2}$, where λ is wavelength of monochromatic (laser) light and θ angle of light incidence ($\theta \geq \theta_c$). Only molecules in a thin layer (200 nm) immediately next to interface can be excited by the evanescent wave i.e. very small sample volume is probed providing excellent sensitivity of the evanescent wave excitation.

Evanescent wave excitation was first used to detect single proteins labeled with 80–100 fluorescent tags.[33] The observation of fluorescently labeled myosin and kinesin molecules,[34] individual ATP turnover reactions[35], three-dimensional imaging of single molecules that are confined in nanometer-sized pores of polyacrylamide gels[36] and imaging of freely moving single molecules in solution at room temperature as they rapidly move into and out of the evanescent field[17] are some examples of the accomplishments this method has allowed at the single-fluorophore level.

Biopolymers at interfaces

The interfacial behavior of biopolymers (notably proteins and nucleic acids) has attracted considerable attention during last few decades. This is most likely due to the importance of their adsorption for both biochemical and biophysical processes, including, for example, the initial steps of atherosclerosis and phagocytosis, as well as the applicability of these phenomena in a range of biomedical applications, such as solid phase diagnostics, drug delivery, extracorporeal therapy, and biosensors. Adsorption of amino acids, peptides, proteins, nucleic acid constituents and nucleic acids on silica surfaces is a very important case of biomolecule adsorption. It is impossible to imagine the modern practice of their

analysis and separation, so widely used in biotechnology, medicine, diagnostics, etc, without high-performance liquid chromatographic (HPLC) methods employing silica stationary phases.[37] Also, the rational design of new biocompatible materials and drug delivery systems needs detailed knowledge on biomolecule adsorption interaction.

Understanding the nature of DNA interactions with silica surfaces is becoming increasingly important as industrial efforts to automate and miniaturize DNA manipulation and purification technologies intensify.[38] Silicon processing technology has advanced to the point where the channels formed in micromachined silicon devices have a wide range of surface properties. Methodologies are available for varying surface potential and charge sign, hydrophobicity and hydrogen bonding capability[39] and it is possible to tailor-make channels in a micromachined device with wanted surface properties to make full advantage of it.
Better understanding of the adsorption of DNA to surface would have impact on many important technologies. The development of the DNA hybridization sensors (which have potential use in sequencing, pathogen detection, mutation detection, etc) and DNA based electric and magnetic molecular devices on silicon wafers[40] (in response to need for miniaturization and acceleration of existing semiconductor devices) are just examples of them. Finally, describing adsorption behavior of DNA in relatively simple systems would also help better understand its behavior in biological, very complex environments.

Single biomolecule experiments

The observation and manipulation of single biomolecules allowed their dynamic behaviors to be studied and provided insight into a wide range of applications such as molecular genetics,[41-43] biochip assembly and biosensor design,[44-50] biophysics,[51-64] and basic separation theories of capillary electrophoresis and liquid chromatography.[65-72]

Real-time imaging of the motion of individual DNA molecules at liquid/solid interfaces provides insights into the fundamental interactions governing the interfacial behavior of DNA. Evanescent wave excitation fluorescent microscopy was used previously

to study the conformational dynamics and adsorption behavior of individual DNA molecules at liquid-solid interfaces.[42,43,68,72]

In single molecule experiments with Lambda DNA, Kang et al.[68] analyzed the motion and adsorption/desorption behaviors of these molecules at the fused-silica/water interface and the C18/water interface as a function of pH and buffer composition. They assessed the driving force for adsorption of individual DNA molecules by the addition of methanol to modulate the strength of the hydrophobic interaction in aqueous solution, and concluded that hydrophobic (nonpolar) interactions of twelve unpaired bases at the ends of Lambda DNA dominate adsorption compared to electrostatic (charge or polar) interactions to initiate adsorption. The retention parameters from these real-time imaging experiments corresponded well with capillary electrophoresis (CE) and liquid chromatography (LC) separations with reference to band broadening and elution times. Li et al.[72] used Lambda DNA as a single molecule probe to study chromatographic retention on various self assembled monolayer surfaces, based on hydrogen bonding ability and hydrophobicity of unpaired purine and pyrimidine bases of ends of Lambda DNA.

The primary goal of here presented work was to examine and compare interfacial behavior of DNAs with single stranded (sticky) ends of different lengths in order to asses the contribution of one unpaired base to specific adsorption of DNAs in aqueous solution at fused silica surface. A flow cell was employed to move DNA solution over fused silica surface at the constant flow and follow individual molecules as they interact with the surface. The behavior and parameters of DNA movement such as adsorption/desorption events, linear velocities and evanescent field residence time of different DNAs were analyzed and compared. We hope that this study can provide further insights into the behavior and important physical parameters of DNA movement at solid/ liquid interface.

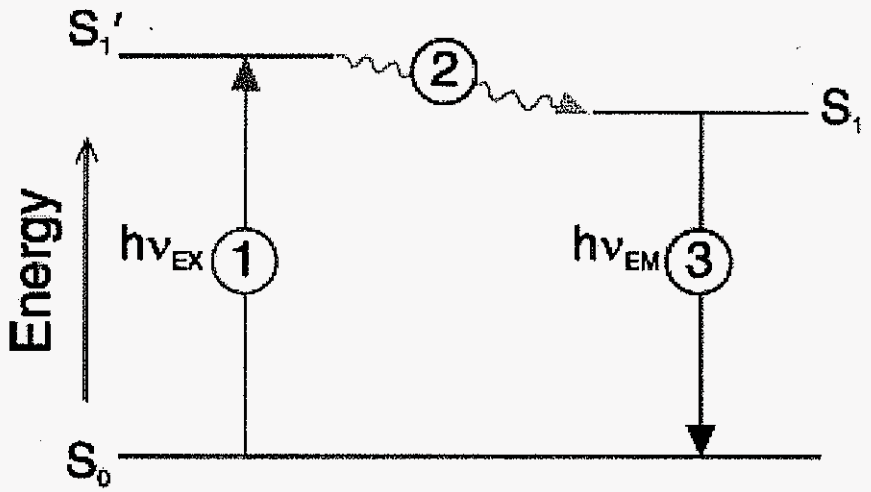

Figure 1.1 Jablonski diagram

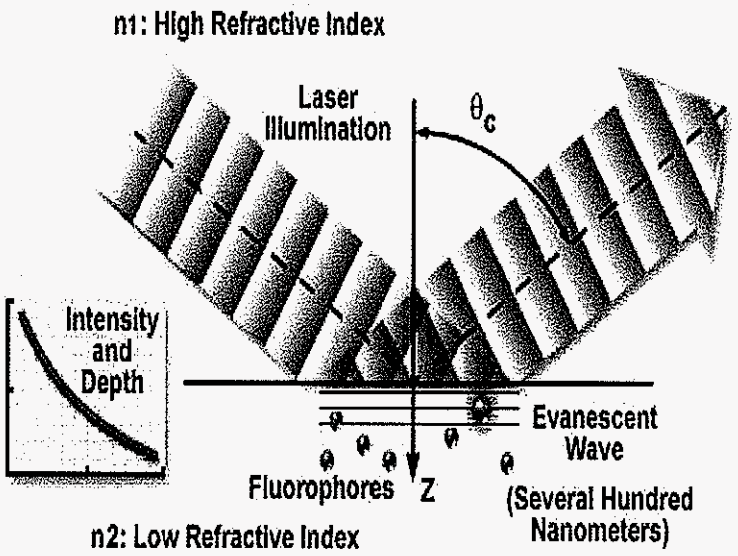

Figure 1.2 Total internal reflection

CHAPTER 2. MATERIALS AND METHODS

Buffer Solutions

Acetate buffer solutions (pH 5.5 and 5.0) were prepared from 1.0 M solutions of acetic acid, sodium acetate, and sodium chloride. ACS grade (or higher) glacial acetic acid, sodium acetate, and sodium chloride (all from Fisher Scientific, Fair Lawn, NJ) were dissolved in ultra pure 18-MΩ water. The molarity and the nominal ionic strength of buffers were 25 mM. All the solutions were photo-bleached using a mercury UV lamp overnight and filtered through a 0.2-μm filter prior to use.

DNA samples

Lambda DNA was purchased from Promega (Madison, WI) and T7 DNA from Alator Biosciences (Madison, WI). Professor Gail Christie (Virginia Commonwealth University) provided us with PSP3 DNA. DNA markers Lambda/HindIII and Lambda Mix Marker (MBI Fermentas, Hanover, MD) were diluted and used according to manufacturers' directions when running gel electrophoresis. All DNA samples were prepared in 10 mM Gly-Gly (Sigma Chemical Co., St. Louis, MO) buffer, pH 8.2. DNA samples were labeled with YOYO-1 (Molecular Probes, Eugene, OR) at a ratio of one dye molecule per five base pairs. DNA samples were prepared at a concentration of 200 pM. For single-molecule imaging, these samples were further diluted to 20 pM with appropriate buffer solutions immediately prior to the start of the experiment.

DNA digestion, hybridizations and gel electrophoresis

We used 1% agarose SeaKem Gold mini gels with ethidium bromide (Cambrex, Rockland, ME) for gel electrophoresis of digested DNA samples. 1xTAE buffer (pH 8.3,

FisherBiotech, Fair Lawn, NJ) was used as running buffer. Electrophoresis time was 45 minutes and applied field 7.7 V/cm. Electrophoresis of whole DNAs was done on 20 cm-long 0.5% agarose gel (casted using SeaKem Gold agarose, 1xTAE buffer and ethidium bromide) at 1V/cm for 36 hours.

PSP3 DNA was digested by BamHI restriction enzyme (Invitrogen, Carlsbad, CA) in the following mixture: 5μl PSP3 (0.1μg/μl), 1μl BamHI (10 units/μl), 2 μl 10xREact®3 Buffer and 13 μl water. Digestion was done at 37° C for 1.5 hours.

Hybridizations were done in a thermo-insulated water bath that had starting temperature 80°C and end temperature 20°C (~24 hour slow cooling). Hybridizations mixtures were in 1x PCR buffer (Qiagen, Valencia, CA) and contained whole DNAs, DNA fragments and oligo-nucleotides in amounts and ratios explained in text. 12-mer nucleotide used in Lambda DNA hybridizations was 5' GGG CGG CGA CCT 3' and 19-mer used in PSP3 hybridizations 5' GGC GTG GCG GGG AAA GCA T 3'.

Flow measurements

Flow monitoring and measurement in the channel was done by using Fluo®spheres (500nm, carboxylate-modified microspheres, yellow-green 505/515, Molecular Probes, Eugene, OR) as tracers. Channel chip was mounted on the stage of Zeiss Axioscope 50 (wide field, epifluorescence microscope), connected to KDS100 syringe pump (KD Scientific, Holliston, MA) and filled with 0.05pM solution of Fluo®spheres in pH 8.2 Gly-Gly buffer. HBO 100 W/2 mercury lamp served as excitation source; FITC filter set was used for selective excitation and collection of fluorescent emission. Movies of flowing solution were taken by PentaMax CCD system (CCD array type EEV CCD-37, pixel size 15x15μm, Princeton Instruments Inc, Trenton, NJ). The camera was working in free run mode with exposure time set at 100 ms. The objective used was 60x Nikon PlanApo (DIC, 1.40 NA, oil type).

Experimental set-up

We used total internal reflection - evanescent field set-up made in the house (Figure 2.1). Single molecules in DNA solutions were followed while moving through a channel in a chip. The chip was placed on the hypotenuse face of a right-angle fused silica prism (UVGSFS, A = B = C = 2.54 cm, Melles Griot, Irvine, CA) and connected to a syringe pump. The chip and the prism were index-matched with a drop of oil (type FF, n = 1.48, R. P. Cargille Laboratories, Inc., Cedar Grove, NJ). The laser beam was focused and directed through the prism and microscope slide (chip) to the channel bottom surface (fused silica slide / DNA sample interface). The angle of incidence was ~66°. The laser beam was totally internally reflected at the channel bottom, and an evanescent field ~150-nm thick was created. Fluorescent molecules within this field could be excited and their fluorescence imaged with a CCD camera. The excitation source was an argon ion laser (Innova-90, Coherent, Santa Clara, CA) operated at 488 nm (Figure 2.2). Extraneous light and plasma lines from the laser were eliminated with an equilateral dispersing prism and optical pinholes (PH1 and PH2) prior to its entry into the observation region. The total laser power just prior to the prism was ~10mW. The microscope objective was a Zeiss 40x Plan-Neofluar (oil, 1.3 NA). It was coupled to the channel chip with immersion oil. Images of the irradiated area at the middle of the channel were recorded by an intensified CCD camera (Cascade, Roper Scientific, Trenton, NJ). The detector element was cooled to -35°C. A 488 nm holographic notch filter (Kaiser Optical System, Ann Arbor, MI) with an optical density greater than 6 was placed between the objective and the CCD camera. The digitization rate of the CCD camera was 1MHz (16 bits). The frame transfer CCD camera was operated in the external synchronization mode. Exposure timing for the CCD camera and laser shutter (S, figure 2.2) was synchronized by a shutter driver/timer (Uniblitz ST132, Vincent Associates, Rochester, NY). The CCD frame rate was 10Hz. The exposure time for each frame was 30 ms. Sequences of images (movies) were acquired for each sample in V^{++} software and analyzed in WinView software (Roper Scientific).

Experimental procedure

Before each single molecule imaging experiment of DNAs, the channel was washed and preconditioned with the appropriate buffer in the following manner: 50μl water, 50μl 0.1M NaOH, 100μl water, 50μl buffer. All rinse steps were done at 0.05ml/h flow rate of syringe pump. DNA solutions were introduced and pumped at 0.04ml/h flow rate

Channel chip fabrication

Chip containing a channel (Figure 2.3) was made using a standard 1x3" fused silica slide (Structure Probe, Inc. West Chester, PA) as a support. 250-μm thick soda lime glass (Nanofilm, West Lake Village, CA) was wet etched and this thin glass plate with 5cm x 80μm x 950μm channel was glued (Norland UV optical adhesive 63, Norland Products Inc., Cranbury, NJ) to fused silica slide. Two holes, 1mm diameter, were drilled in the fused silica slide and capillary tubings were connected to chip by capillary connectors (Nanoports, Upchurch Scientific, Inc., Oak Harbor, WA) also glued to chip. The prism and the chip were fixed in a prism/chip holder (Figure 2.4) to prevent sliding and moving of the chip during injections and imaging experiments.

Wet etching

The microchannel in thin glass plate was made using standard wet etching procedure. A photomask with a channel drawn on a transparency sheet was piled on a photoresist-coated glass plate (soda lime, AZ1518, 0.010" thick, Nanofilm, Westlake Village, CA). The plate with transparency was exposed to UV light from a lamp for 30 minutes. After UV exposure, the plate was: soaked in developer solution (AZ 915 MIF Developer, Clariant Corp., Charlotte, NC), water rinsed, soaked in chrome etchant (CEP-200 Micro-Chrome Etchant, Microchrome Technology Inc., San Jose, CA), water rinsed, soaked in $HF:HNO_3:H_2O$ =

20:14:66 with shaking for 10 minutes, water rinsed, soaked in acetone, water rinsed, soaked in chrome etchant and water rinsed.

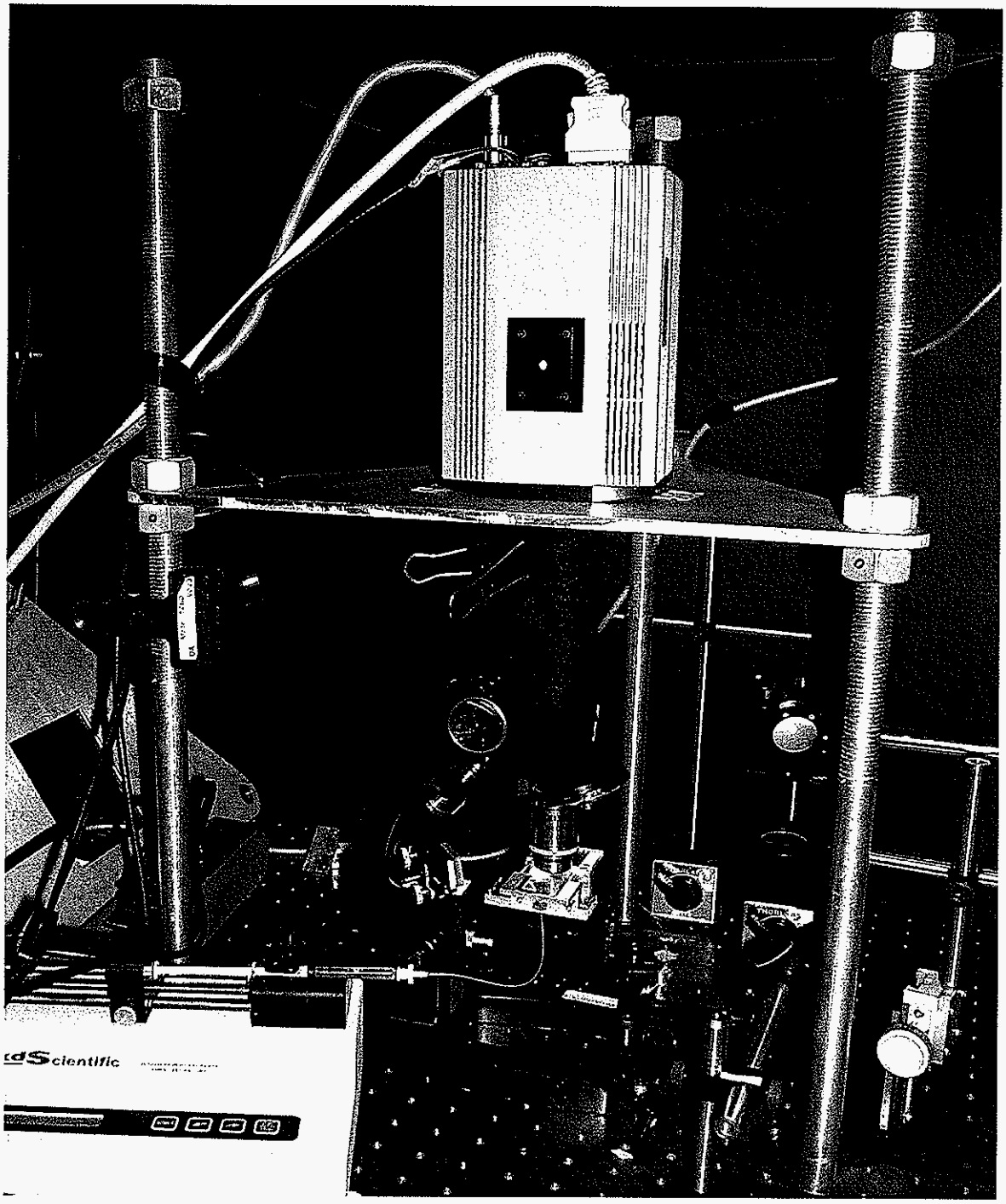

Figure 2.1

Total internal reflection - fluorescence microscopy (TIR-FM) set-up.

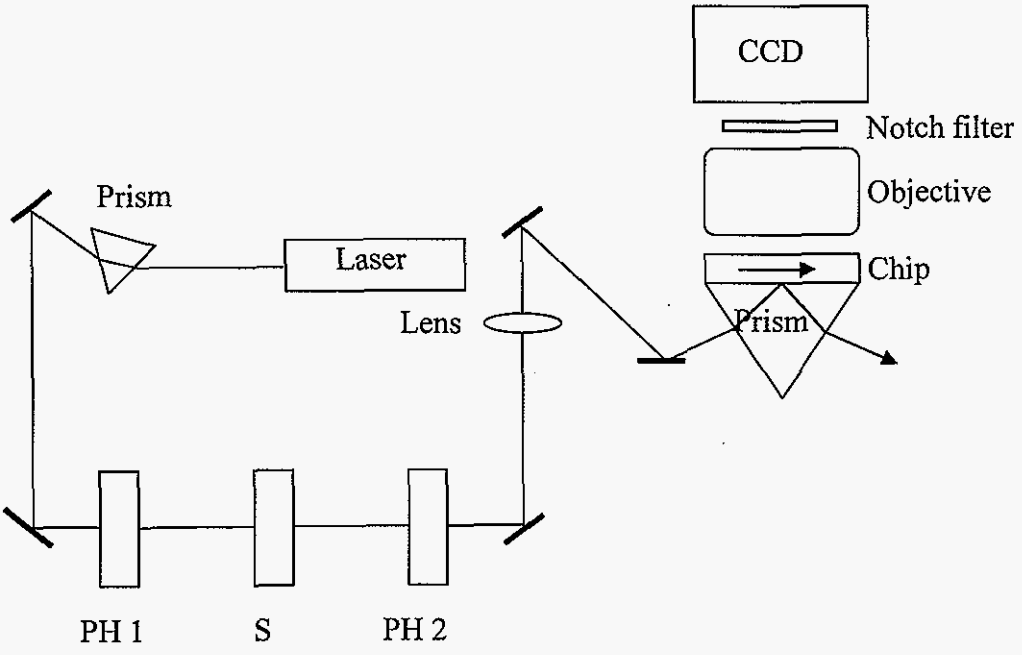

Figure 2.2

TIR-FM set-up scheme.

PH 1 and PH 2 are pinholes, S is a mechanical shutter.

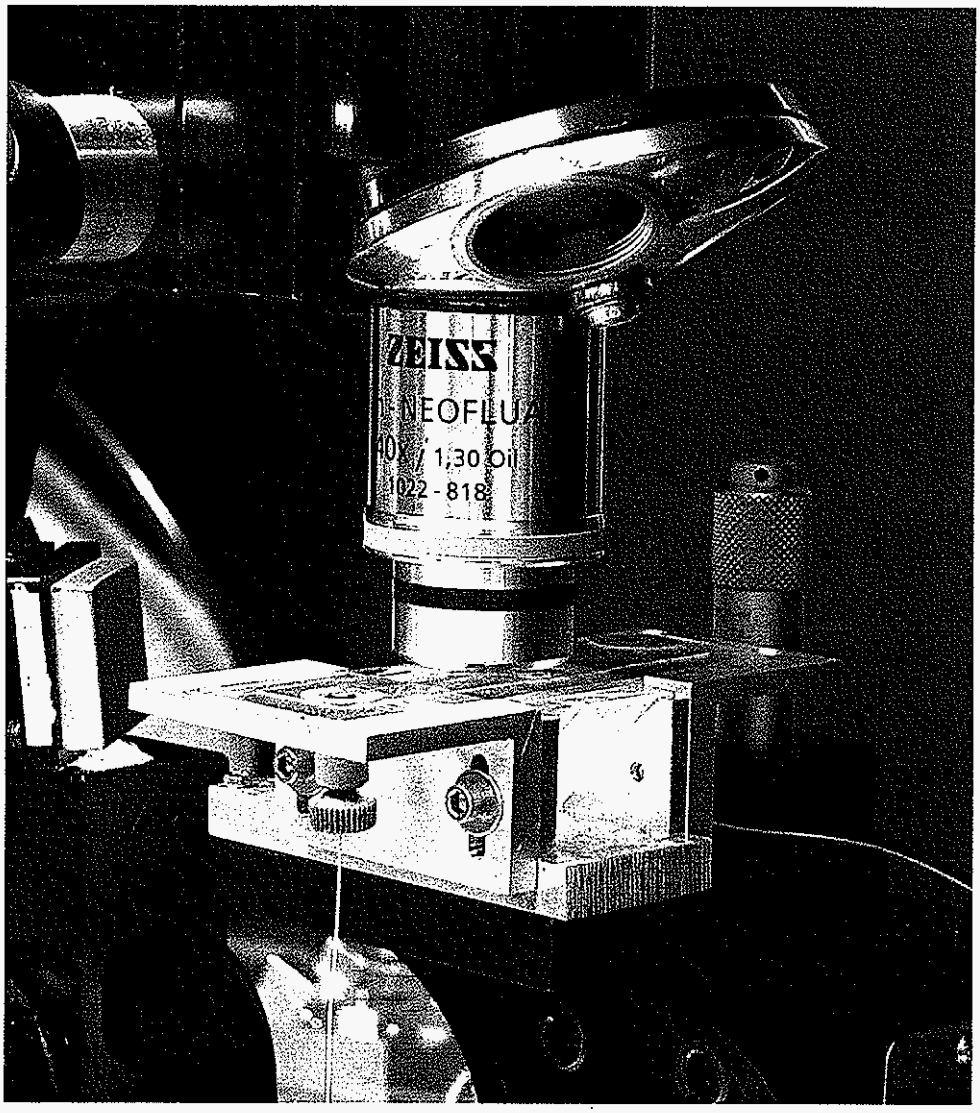

Figure 2.3

Chip-prism holder with microscope objective in place.

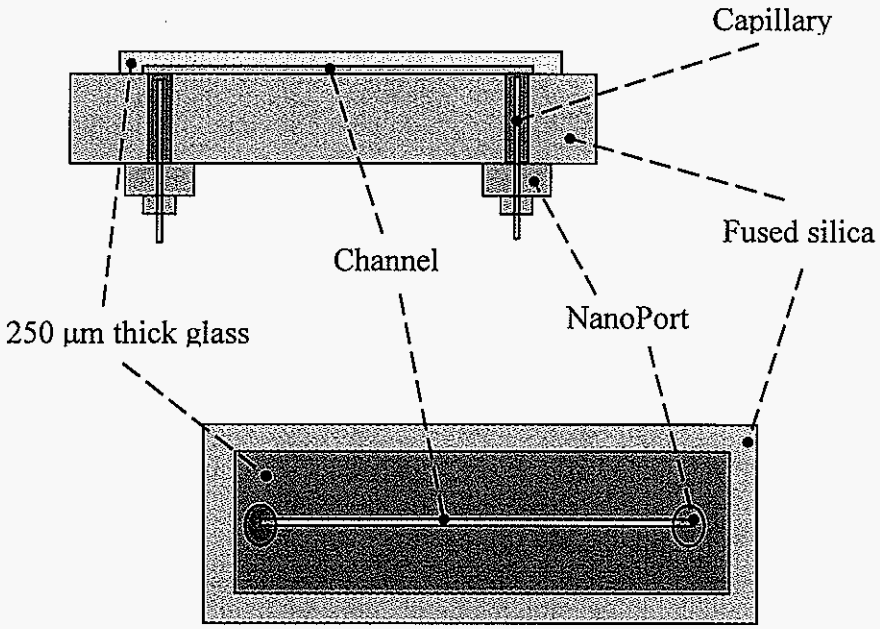

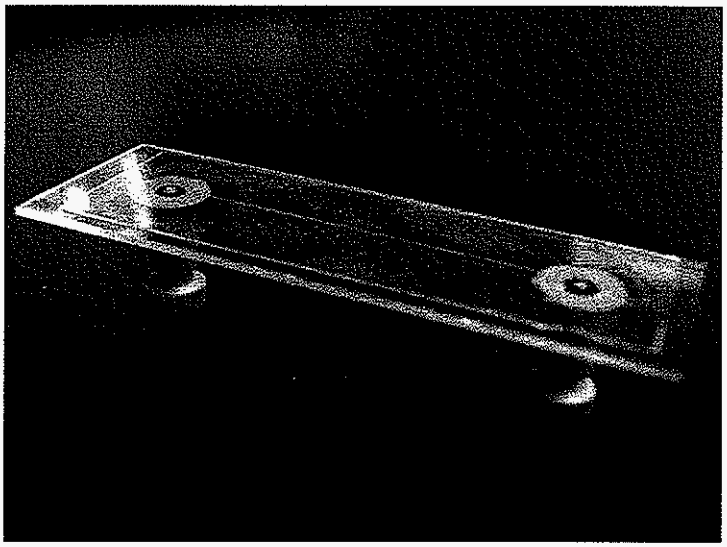

Figure 2.4

Scheme (top) and photo (bottom) of channel chip.

CHAPTER 3. RESULTS AND DISCUSSION

Flow control

Constant flow rate in the channel allowed us to directly compare parameters obtained from single-molecule measurements of various DNAs at water/fused silica interface. A syringe pump was employed to establish the constant flow. A set of control experiments was performed to confirm stability and reproducibility of the generated flow.

The linear flow rate was determined by tracing fluorescent microspheres in the microchannel. Velocities of microspheres were determined by using streak method.[65] We measured the lengths of bright traces that microspheres made by moving across the field of view in a frame of a movie for which the exposure time was 100 ms (Figure 3.1). In laminar flow, which was established in the microchannel, the flow profile is parabolic (Poiseuille profile), being the fastest in the middle and the slowest at channel walls. For the measurement, we set the image focus in the middle of the microchannel so the sharply focused traces had the longest length (x) and the shortest width (y) (Figure 3.1 and 3.2). Some of the fastest microspheres were out of focus (Figure 3.1 B) because the depth of field of the used microscope objective was less than 1 μm, and did not completely cover fast-moving layer in the middle of the channel. We measured traces that were up to 20-pixel wide in order to avoid sampling layers farther from the center and minimize the error of the measurement.

The maximal linear velocity, calculated from 5 sets of measurements (Figure 3.2) was v_{max} = 176 ± 5 pixels/frame = 282 ± 8 μm/s, and was very close to the value calculated from the set flow rate and channel dimensions (v_{max} = 2F /A = (2 x 0.04 ml/h) / (80 x 950 μm^2) = 292 μm/s = 183 pixels/frame). The flow in the channel was reproducible and constant (within the above range) as we confirmed in repeated 20-minute-long-runs. Before each run syringe was changed and flow restarted, as it was done in the actual experiments with DNA solutions.

DNA size

We used three large double stranded DNAs originating from Lambda (48.5 kb), T7 (39 kb) and PSP3 (30.6 kb) phages in our experiments (Figure 3.3). Sizes of these DNAs provide an excellent signal-to-noise ratio for single molecule imaging experiments since each DNA molecule is labeled with many fluorescent YOYO-1 dye molecules (bp:dye = 5:1).

Also, their macromolecular sizes make them more amenable for evanescent wave excitation single-molecule imaging in free solution because their diffusion is slower compared to small molecules. The diffusion coefficients of small molecules in water, such as rhodamine 6G ($D = 2.8 \cdot 10^{-6}$ cm^2/s)[62] are large, so they stay in the evanescent-field layer (EFL) only for short periods of time (hundreds of microseconds). It is not possible to follow individual small molecules by taking series of consecutive images even at fastest frame rates. For large molecules such as DNA ($D \sim 10^{-9}$ cm^2/s) each molecule can be tracked over many frames during hundreds of milliseconds.[68,72]

Hybridization experiments

PSP3 and Lambda DNA are double stranded DNAs with unpaired or single stranded ends. There are 19 bases at both ends of PSP3 DNA, and 12 bases at both ends of Lambda DNA that are not hydrogen-bonded to their complements. The two unpaired single stranded ends of a DNA are actually complementary and they hybridize when they come close to each other. Because of this, they are called sticky ends. We used this property and confirmed the lengths of sticky ends in a set of hybridization experiments. Large DNAs were digested into smaller fragments, hybridized, and analyzed by standard slab gel electrophoresis.

From restriction map of PSP3 DNA with BamHI restriction endonuclease (Figure 3.4) it can be seen that fragments with unpaired 19-base ends are 3 kb and 7.7 kb long. When sticky ends of these relatively short DNAs hybridize to each other, a new bigger, 10.7 kb DNA is formed (Figure 3.5, left). If an oligonucleotide, with the sequence identical to the one

of the unpaired ends (we used 19-mer identical to sticky end of 3 kb DNA in the experiment), is present in the hybridization mixture it will compete with 3 kb DNA to hybridize to the other sticky end (to 7.7 kb fragment). Therefore, less 10.7 kb DNA should be formed or not formed at all (Figure 3.5, right). Gel electrophoresis of these DNA hybridization mixtures shows clearly if hybridization between 3 kb and 7.7 kb DNAs occurred (Figure 3.6, right lane: 10.7 kb band present and 3 kb and 7.7 kb bands absent) or not (Figure 3.6, middle lane: 10.7 kb band absent and 3 kb and 7.7 kb bands present).

Hybridization of DNA fragments with sticky ends happened within an hour even at room temperature (Figure 3.7, lane 1) and its efficiency was 100 % when DNA mixture was incubated at higher temperature for 24 hours (Figure 3.7, lane 3). The analysis of hybridization mixtures with oligomer showed that 19-mer prevents efficient formation of 10.7 kb (Figure 3.7, lane 4). These results confirmed the presence of 19-base long ends of PSP3 DNA. In analog hybridization experiments of Lambda/HindIII fragments (Figure 3.6, left lane), we confirmed the presence of 12-base sticky ends of Lambda DNA. Lambda/HindIII digest, which was incubated for 24 hours, showed hybridization of 4.3 kb to 23 kb fragment (Figure 3.8, lane 5). 4.3 kb band in lane 5 was less intense compared to the 4.3 kb band in lane 6 of denatured or separated fragments. Also, 12-mer oligonucleotide was hybridized to 4.3 kb fragment, recovering the intensity of 4.3 kb band (Figure 3.8, lane 2). The hybridization was especially efficient for higher oligo to DNA ratios (Figure 3.8, lanes 3 and 4).

Hybridization of 4.3 to 23 kb DNA was not 100 % efficient (4.3 kb band would be absent in that case from lane 5, Figure 3.8) in contrast to hybridization of 3 and 7.7 kb DNAs (lane 3, Figure 3.7). The hybridization of intact (whole) 30 kb PSP3 DNAs also showed lower hybridization efficiency (Figure 3.7, lane 5) compared to shorter 3 and 7.7 kb DNAs. The higher hybridization efficiency of shorter DNAs can be due to their higher diffusion coefficients, therefore higher number of encounters and hybridization events. The other reason for the different hybridization efficiencies of long and short DNAs could be different availability or accessibility of the sticky ends of the long compared to the short chain. DNAs

at pH $\geq$ 7 are random coils and it is possible that ends of longer chains get trapped within coiled structure more often than in shorter chains.[75] A hybridization experiment of the whole PSP3 DNA and 19-mer nucleotide did not confirm this (Figure 3.7, lane 6) because we saw similar relative amounts of hybridized and unhybridized bands in DNA-oligo mixture pre-digested (Figure 3.7, lane 4) and post-digested (Figure 3.7, lane 6). Oligomers have accessed their complementary sticky ends at both 30 kb and 7.7 kb DNAs, making very similar amounts of hybrids with shorter and longer DNA. This is most probably due to the small size of oligomers that enables them to reach the sticky ends in the coil of 30 kb DNA (or 23 kb, in case of Lambda/HindIII digest), in contrast to big, 30 kb DNA "hybridization probe" (or 4.3kb for Lambda/HindIII digest).

Single-molecule experiments

DNAs in basic and acidic buffers

The single molecule experiments with three DNAs containing different sticky ends at water/fused silica interface showed strong pH dependent behavior as reported previously for Lambda DNA.[68,72] At pH 8.2, individual DNA molecules were free, and appeared as random coils that changed their shapes while flowing carried by the bulk flow. Molecules appeared and disappeared at random locations at surface in the field of view. Individual molecules of all three DNAs could be followed (imaged) in similar number of consecutive frames before they diffuse out of evanescent field layer (EFL) and become invisible. Histogram of EFL residence times for 50 molecules of each DNA (Figure 3.9) shows that single molecules could be followed up to 12 frames (1.2 seconds).

At pH 5.5, molecules were also moving across the surface, but the EFL residence time generally increased (Figure 3.10) compared to the EFL residence time at pH 8.2. The increase in EFL residence time was especially noticeable for some PSP3 and Lambda molecules that were followed in the EFL twice as long as at pH 8.2. Also, at pH 5.5, some

molecules showed reversible adsorption and desorption from surface. These molecules adsorbed at random locations of observed surface and most of them stayed immobilized for 200-300 ms (Figure 3.11), but longer immobilizations (up to a second, for PSP3 molecules) were seen too. We found that 12–16% of followed PSP3 molecules and 4–6% of Lambda DNA molecules underwent adsorption/desorption, whereas DNAs in T7 sample did not show this kind of behavior.

At pH 5.0, DNA molecules moved across the surface. Some molecules attached by one of the ends and stretched, whereas others left the field of view either carried by the flow or diffusing out of EFL. It was not possible to distinguish moving molecules of different DNA samples because they all looked like either short rods or coils. But, after adsorption, stretched strands had lengths directly proportional to the size of corresponding DNAs (Figure 3.12). Molecules of all three DNA samples were showing permanent adsorption at surface. The adsorption of DNAs at this pH was not reversible so that once attached DNA moecules stayed on the surface during the whole time of the imaging experiment (few minutes).

The observed behavior of DNAs at varying pH was explained by electrostatic, hydrophobic, and hydrogen-bonding interactions of varying degrees.[68,72] At high pH, both fused silica and DNA are negatively charged so the strong repulsive electrostatic force dominates their interaction and no adsorption is observed. As pH decreases below pK_a of silica (~6),[73,74] silanoate groups of surface protonate, electrostatic repulsion between DNA and surface reduces and DNAs approach closer to the surface. This leads to increase in EFL residence times for DNAs at pH 5.5 compared to pH 8.2. At pH 5, hydrophobic interactions and hydrogen bonding of unpaired purine and pyrimidine bases of DNA's ends initiate DNA adsorption to surface, so that DNAs are attached by the end and stretched. The effects of these interactions are confirmed by the strongest surface-DNA interactions in the case of DNA with the longest sticky ends (PSP3). PSP3 had longer EFL residence time and more frequent and longer adsorption/desorption events compared to Lambda with shorter sticky ends, and T7 DNA without sticky ends. T7 DNA adsorbs by its end and stretches at pH 5 due

to dye intercalation effects. Dye binding causes partial unwinding of the T7 DNA ends so that this molecule also has few unpaired bases at the ends of the chain.[76]

Velocities of DNAs

The measurements of linear velocities of three DNAs at pH 8.2 showed no obvious difference between different DNAs. They moved at 13 ± 2 pixels/frame (=13 · 0.14μm / 0.1s = 18 ± 3 μm/s). In contrast, at pH 5.5 all three DNAs' velocities were in the broad range from 3 to 14 pixels/frame, as found from linear velocities of hundred molecules of each DNA sample (Figure 3.13). Even though all three DNA samples showed molecules with velocities from the whole range, the distributions of the velocities for different DNA samples were different. PSP3 sample had the slowest moving molecules and velocity of 8 pixel/frame as most frequent. Lambda sample's most frequent velocity was 9 pixels/frame and T7 sample had most molecules moving at 12 pixels/frame. The average calculated velocities also showed a decrease going from T7 to PSP3: 10 ± 3, 9 ± 4, and 8 ± 4 pixels/frame. Again, slower velocities of DNAs with longer sticky ends indicate and confirm their stronger attractive interactions and hence retention at fused silica surface.

DNA conformation dynamics at interface

The analysis of differences in adsorption/desorption, EFL residence (follow) times and linear velocities between Lambda, PSP3 and T7 DNAs at pH 5.5 reflect the differences in the length of their unpaired ends in bases. The longer the sticky end, the higher the affinity of DNA for surface. As in the case of hybridization of larger and shorter DNAs, the difference in diffusion coefficients and sticky end availability are important factors for DNA-surface interactions. The differences in sizes of these DNAs do not contribute much to differences in diffusion at pH 8. 2 since all three DNAs stay close to surface during similar periods of time (Figure 3.9). If diffusion factor is excluded as a parameter, than sticky ends

of 30 kb DNA (PSP3) are more available outside the coil than the ends of 50kb DNA (Lambda) This causes three times more adsorption/desorption events at pH 5.5 for PSP3 DNA (12-16% of all molecules) than for Lambda DNA(4-6% of all molecules), and not 1.5 times as it could be expected from the ratio of their sticky end lengths. The absence of direct proportionality between sticky end length and affinities for the surface could be explained by different conformational dynamics of DNA molecules of different sizes . Conformation of a molecule, its orientation and availability of sticky ends are all the factors that determine how the molecule will interact and move across the surface. This was especially obvious in single molecule imaging experiments at pH 5. Part of the observed molecules simply moved along the surface and left EFL after a while, whereas others attached by the sticky end when it got in contact with surface and stretched.

Conclusion

This work showed application of total internal reflection evanescent field fluorescence microscopy (TIRFM) to study intermolecular interactions at water-fused silica interface at single-molecule level. Real-time molecular motion at the interface was recorded to reveal adsorption behavior and conformational dynamics of three long DNAs with sticky ends of different lengths. Parameters of DNA molecule motion at the interface, such as evanescent field residence time, linear velocity and frequency of adsorption/desorption events were measured to asses the relative affinities of oligonucleotides of different lengths for fused silica surface. The general trend of stronger interaction of longer sticky ends with surface confirmed hydrophobic interactions and hydrogen bonds of unpaired bases as driving force of DNA adsorption at fused silica at pH 5. At this pH the interaction of DNA with surface is stronger for DNA containing the longest sticky ends. Different conformational dynamics and availability of sticky ends of DNAs of different lengths prevented seeing direct proportionality of affinities of DNAs for surface and the length of their sticky ends. A study, in which a DNA of constant size with sticky ends of various lengths would be used, should

provide more precise information on the contribution of one unpaired base to adsorption of DNA at water/fused silica surface. The effect of the size i.e. the length of a DNA chain to adsorption or the availability of the ends could be described in more detail from a study in which DNA size would vary and the length of sticky end is kept constant. Also, by following individual DNA molecules at fused silica/water interface we could recognize their different conformations and ways of approaching and interacting with the surface.

We demonstrated the ability of single molecule approach to recognize subtle differences in behavior of individual molecules of heterogeneous sample that would be obscured by ensemble-averaged measurement. Our study provides information that further elucidates intermolecular interactions and conformations of DNA at liquid/solid interface. Such information may prove valuable for chromatography studies as well as for design of DNA hybridization sensors (microarrays) and drug delivery systems.

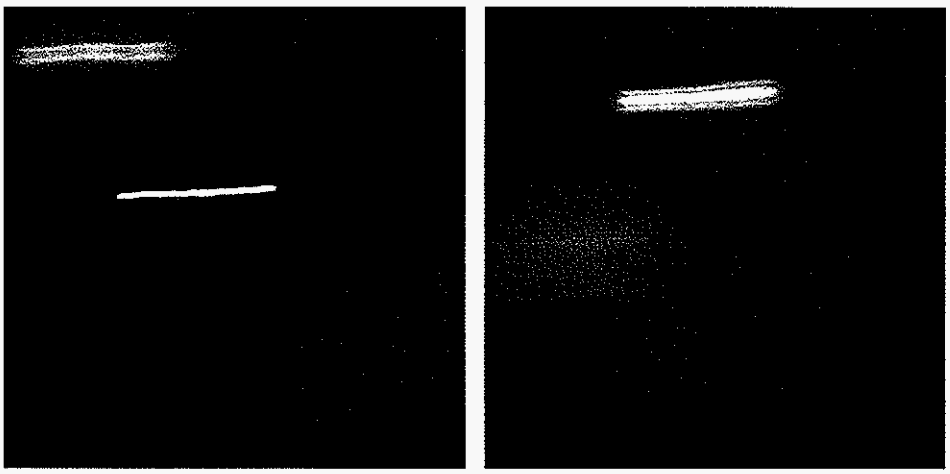

A B

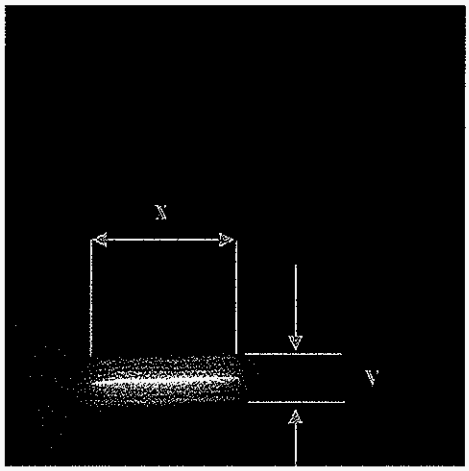

C

Figure 3.1

Examples of microsphere traces made during 100ms. Three frames (A, B, and C) from a movie are shown. The widths (y) and lengths (x) of traces in pixels are: 9 and 175 (A), 31 and 174 (B), and 55 and 164 (C). The size of the pixel is approximately 0.16 x 0.16 μm as measured by microscope stage micrometer.

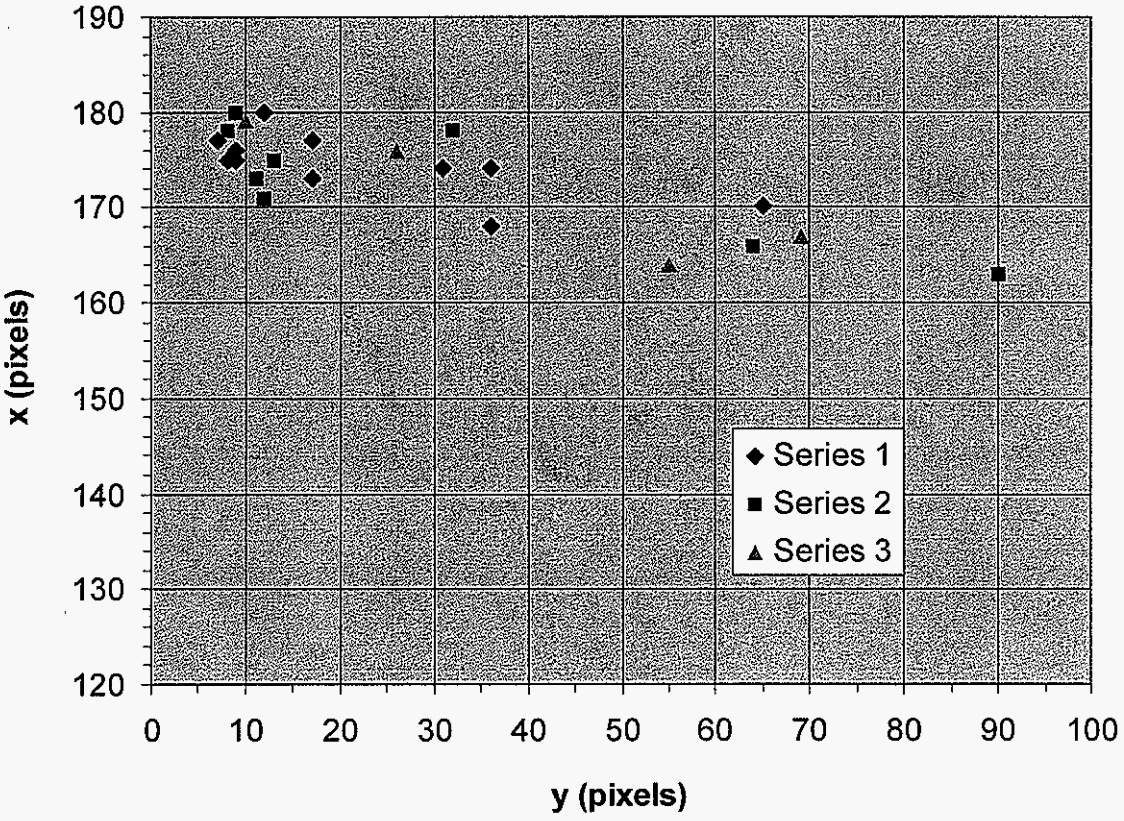

Figure 3.2

Trace length (x) versus trace width (y). Each series of measurement is taken from a 200-frame movie. A data point was measured for a single particle trace as shown in Figure 3.1 C.

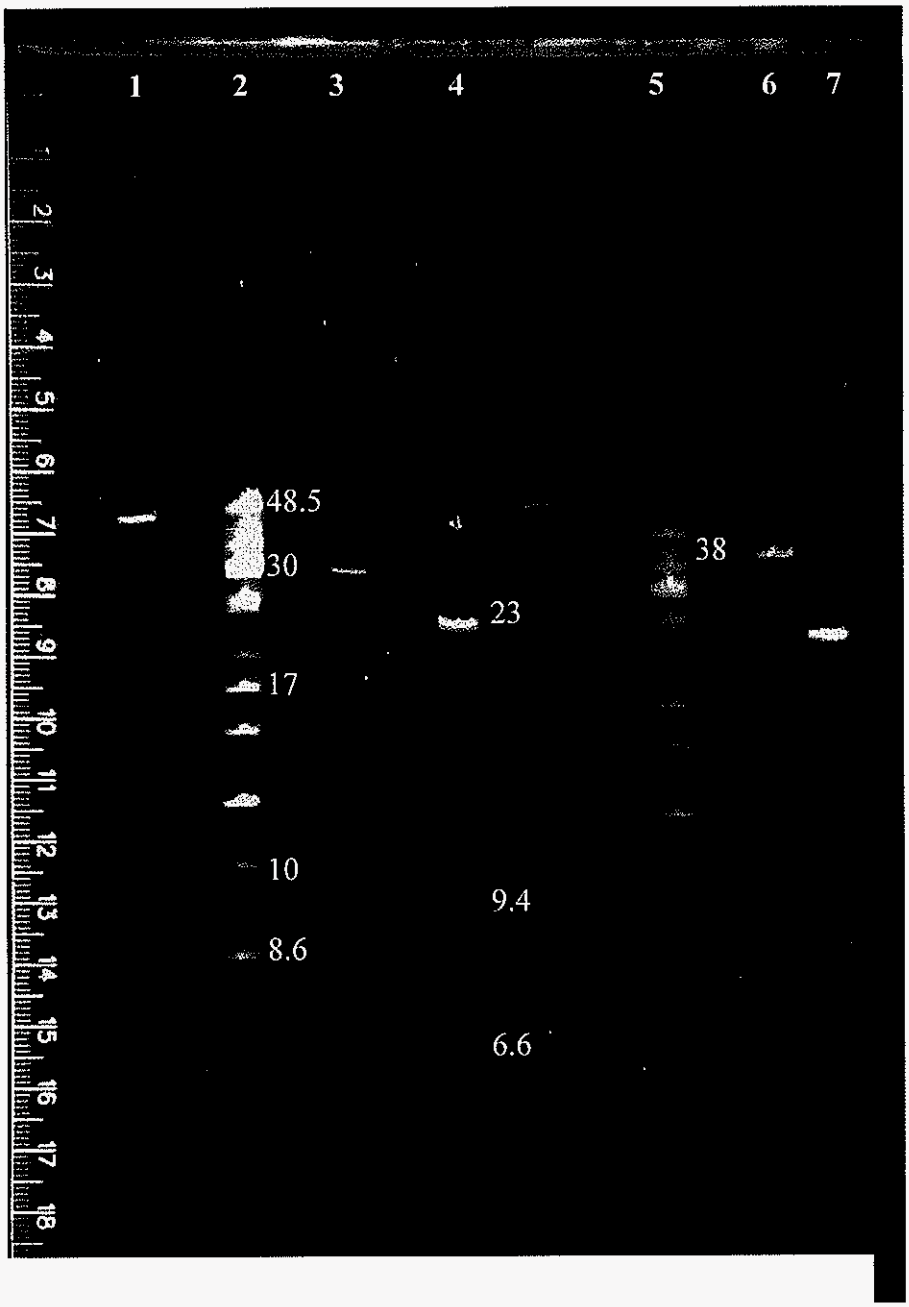

Figure 3.3

Gel electrophoresis of DNA samples: Lambda - 48.5 kbp (lane 1), Lambda Mix DNA standards (lanes 2 and 5), PSP3 DNA – 30.6 kbp (lane 3), Lambda/HindIII DNA standards (lanes 4 and 7), T7 DNA – 39 kbp (lane 6). The numbers on the right of bands are their sizes in kilo-base pairs (kbp).

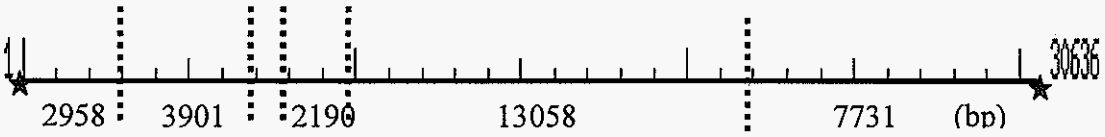

#	Ends	Coordinates	Length (bp)
1	BamHI-BamHI	9848-22905	13058
2	BamHI-(RightEnd)	22906-30636	7731
3	BamHI-BamHI	2959-6859	3901
4	(LeftEnd)-BamHI	1-2958	2958
5	BamHI-BamHI	7658-9847	2190
6	BamHI-BamHI	6860-7657	798

Figure 3.4

Restriction map of PSP3 DNA for BamHI restriction endonuclease (top) and the list of restriction fragments(bottom).

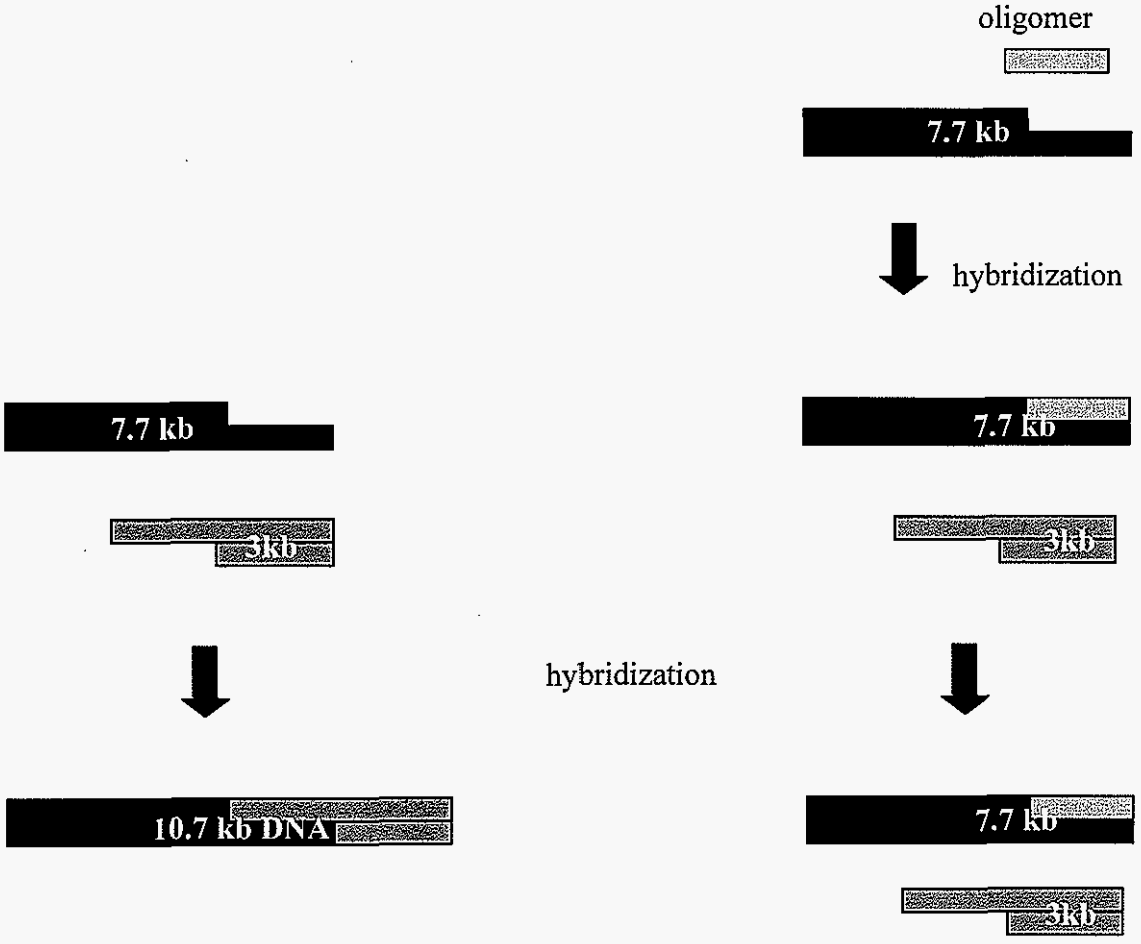

Figure 3.5

The scheme of hybridization experiments with PSP3 DNA fragments. The hybridization conditions are described in the Materials and Methods section.

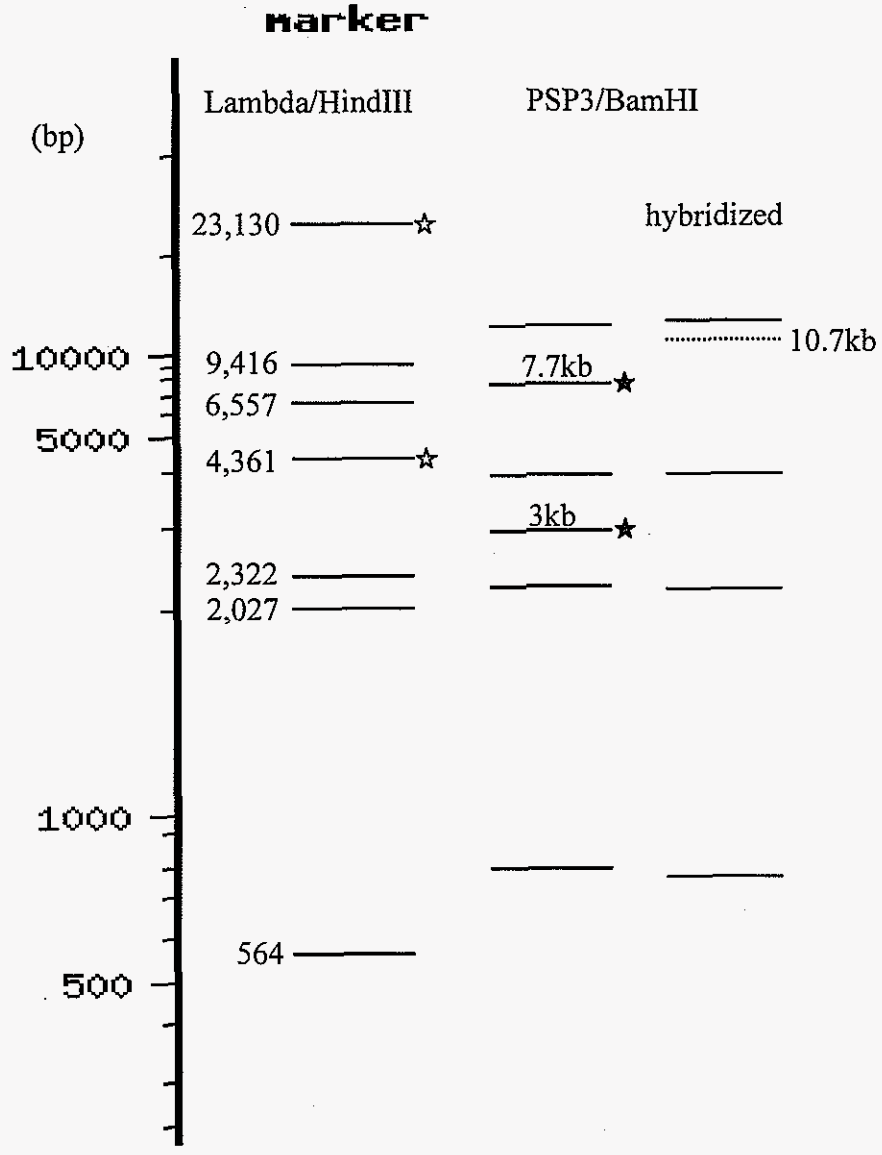

Figure 3.6

Bands of DNA restriction fragments on 1% agarose gel after electrophoresis. Left lane shows bands of Lambda DNA cut by HindIII (23 kbp fragment and 4.3 kbp fragment unhybridized). PSP3/BamHI bands are shown in the middle lane (3 kbp and 7.7 kbp fragments unhybridized) and left lane (3 kbp and 7.7 kbp fragments hybridized). Stars mark fragments with unpaired ends.

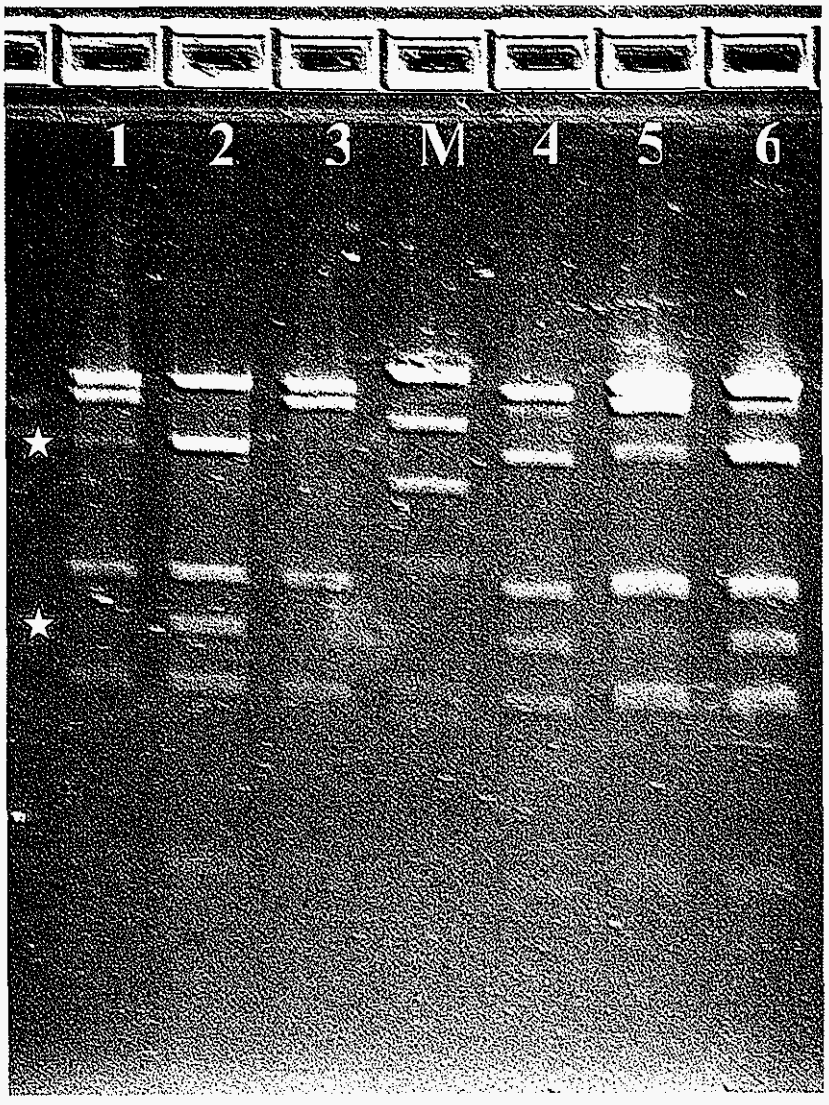

Figure 3.7

Gel electrophoresis of PSP3/BamHI hybridization mixtures: one hour at room temperature (lane 1); 10 min at 65°C, 5 min at 0°C (lane 2); 24 hours (lane 3); DNA standards (lane M); with oligomer, 24 hours (lane 4); intact PSP3 DNA, 24 hours, than digested (lane 5); and intact PSP3 with oligomer, 24 hours, than digested (lane 6). All 24-hour-incubations were started at 80°C and gradually cooled to room temperature in 24 hours. (Stars are at the level of bands of fragments with sticky ends for easier recognition)

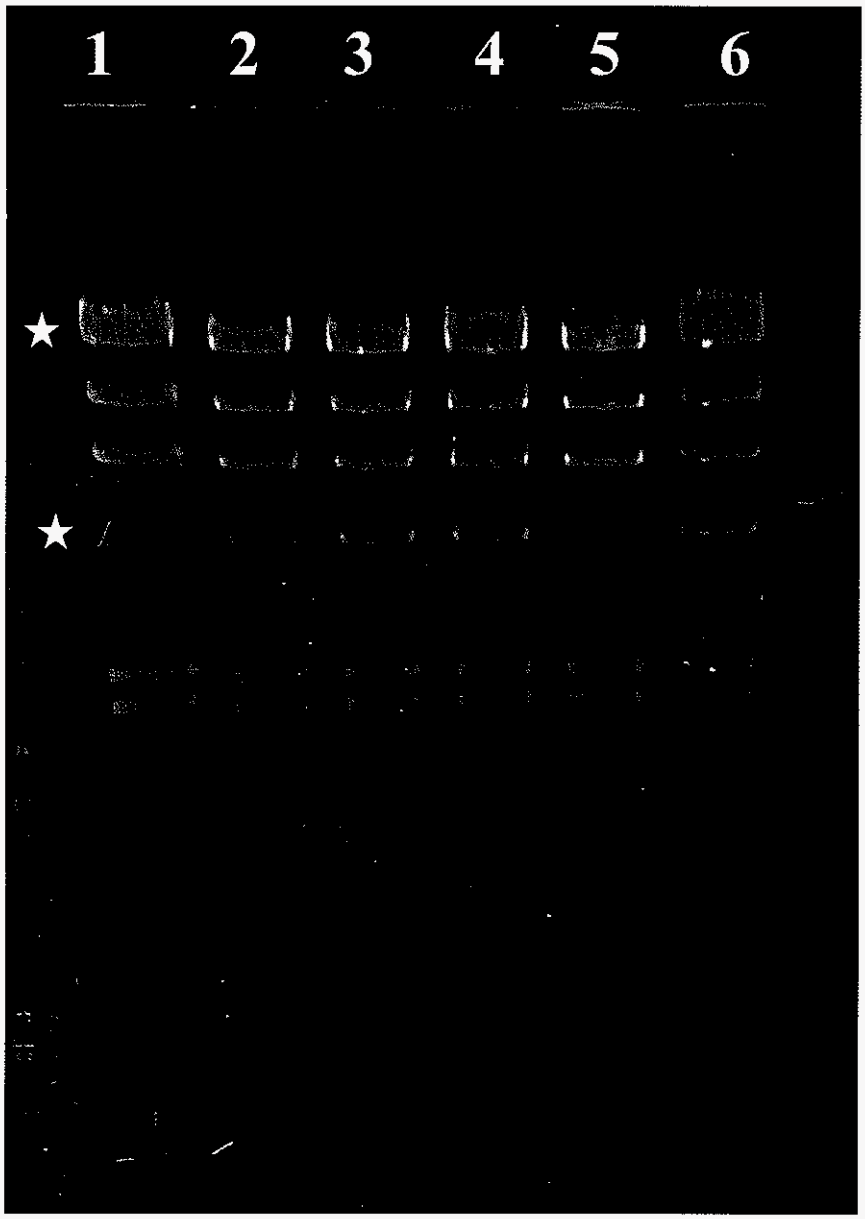

Figure 3.8

Gel electrophoresis of Lambda/HindIII hybridization mixtures: room temperature, 1 hour (lane 1); with oligomer, 24 hours, oligomer: DNA = 1:1 (lane 2), 2:1 (lane 3), 4:1 (lane 4); 24 hours (lane 5); 10 min at 65°C, 5 min at 0°C (lane 6). All 24-hour-hybridization incubations were started at 80°C and gradually cooled to room temperature in 24 hours.

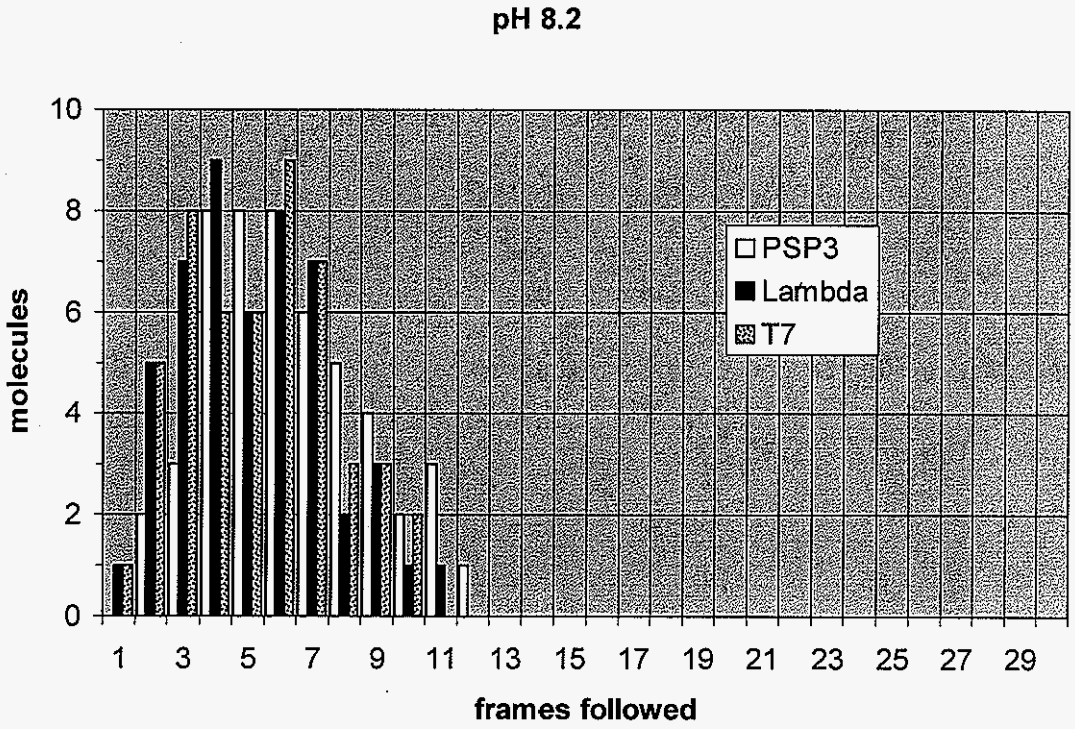

Figure 3.9

Distribution of times individual molecules were followed for three DNA samples (50 molecules of each) at pH 8.2. "1 frame" follow time means that a molecule was followed in two consecutive frames or during 100 ms.

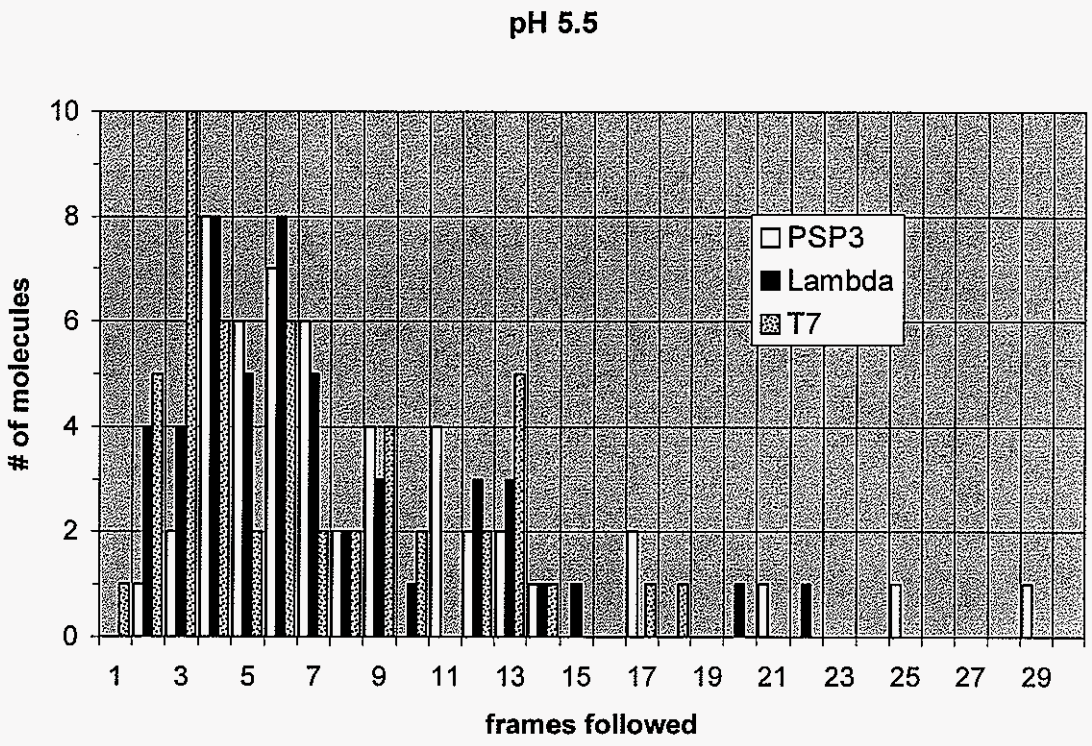

Figure 3.10

Distribution of times individual molecules were followed for tree DNA samples (50 molecules each) at pH 5.5. "1 frame" follow time means that a molecule was followed in two consecutive frames or during 100 ms.

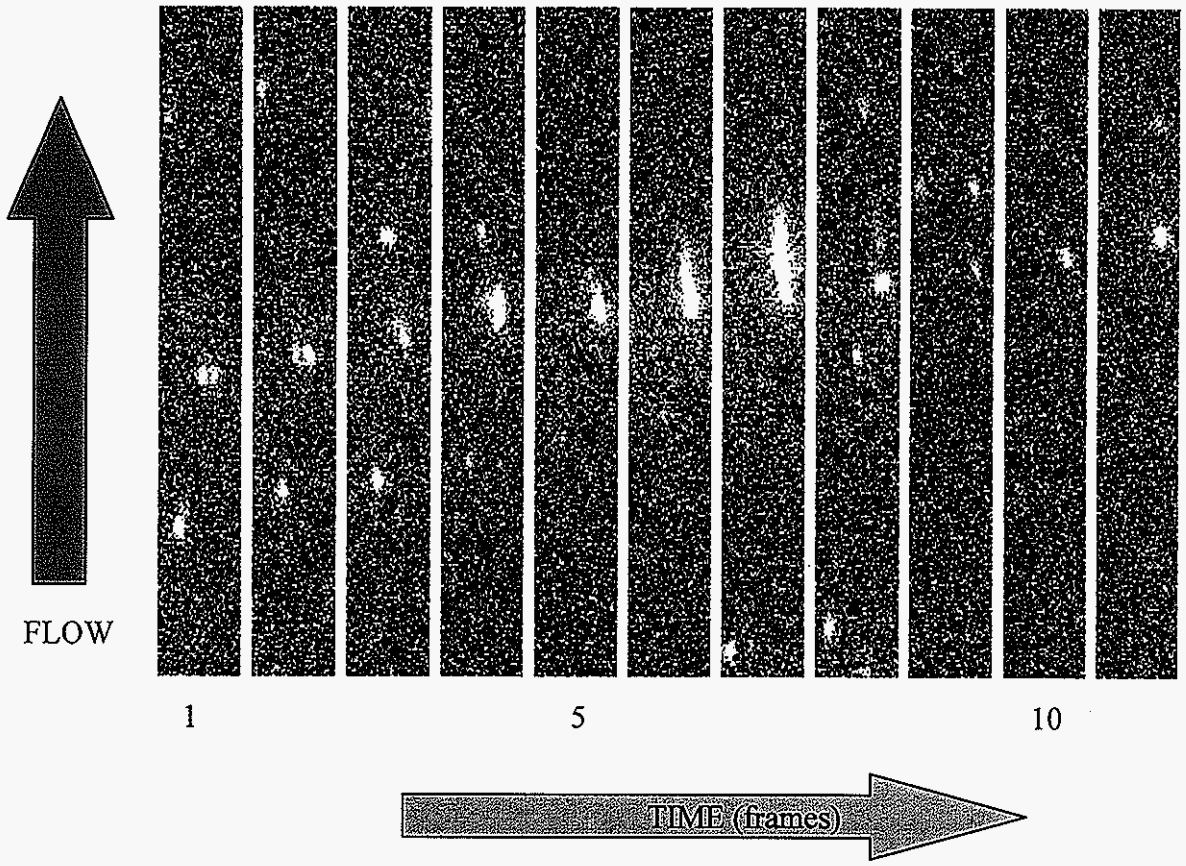

Figure 3.11

The adsorption-desorption process of a single DNA molecule (immobilized and stretched from frame 4 to frame 6). DNA came to a surface spot, stretched in the direction of the solution flow and stayed adsorbed at the same spot for 3 consecutive frames (~300 ms). In contrast, DNA underneath the adsorbed molecule moves constantly from frame to frame.

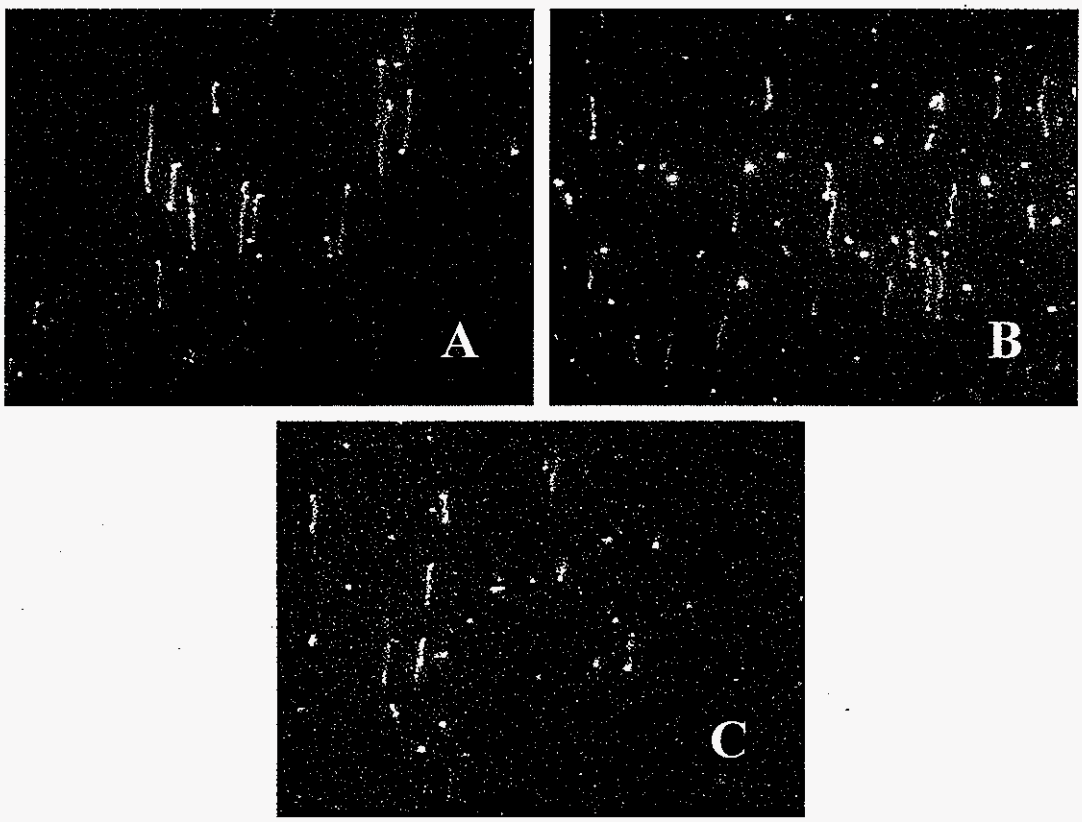

Figure 3.12

Single DNA molecules at fused silica surface in acetate buffer, pH 5: Lambda (A), T7 (B) and PSP3 (C). The direction of flow was vertical. The ratio of the lengths of stretched DNAs is 3:4:5 = PSP3:T7:Lambda

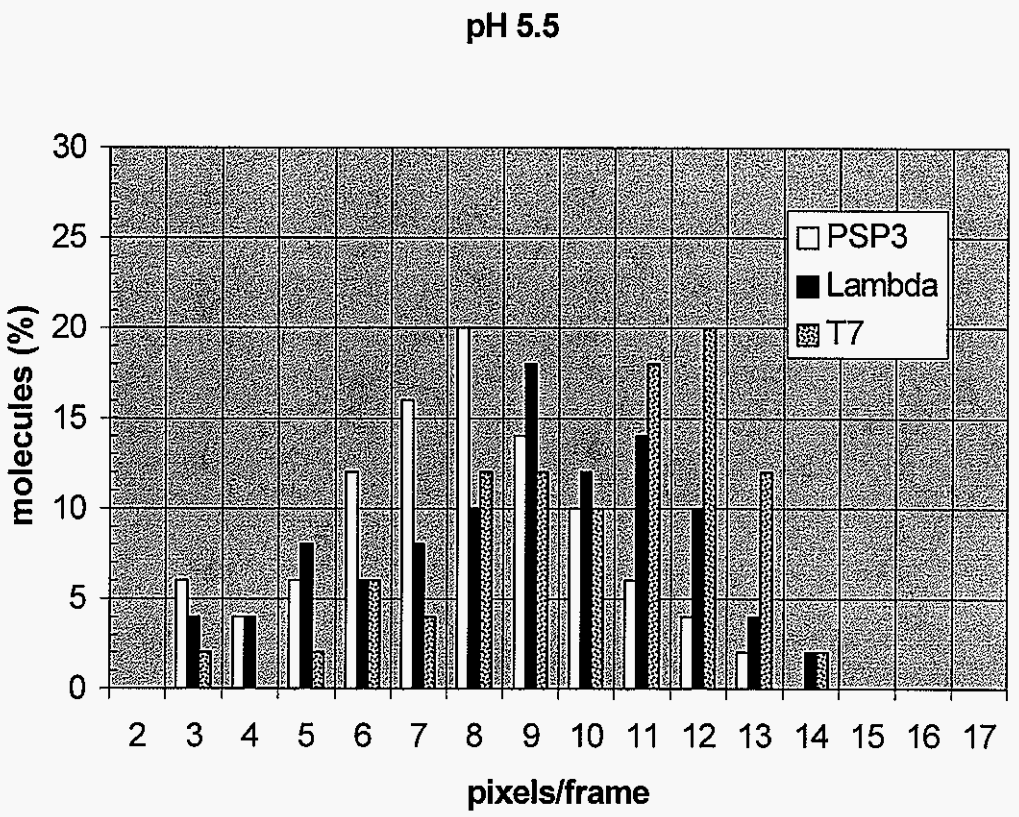

Figure 3.13

The distribution of linear velocities of three DNA samples (100 molecules of each) at pH 5.5

REFERENCES

(1) Xie, X. S.; Dunn, R. C. *Science* **1994**, 265, 361-4

(2) Barnes, M. D.; Whitten, W. B.; Ramsay, J. M. *Anal. Chem.* **1995**, *67*, A418–23

(3) Rigler, R. J. *Biotechnol.* **1995**, *41*, 177-86

(4) Keller, R. A.; Ambrose, W. P.; Goodwin, P. M.; Jett, J. H.; Martin, J. C.; Wu, M. *Appl. Spectrosc.* **1996**, *50*, 12-32A

(5) Xie, X. S. *Acc. Chem. Res.* **1996**, *29*, 598-606

(6) Nie S. M.; Zare R. N. *Ann. Rev. Biophys. Biomol. Struct.* **1997**, *26*, 567-596

(7) Meixner, A. J. *Adv. Photochem.* **1998**, *24*, 1-59

(8) Xie, X. S.; Trautman J. K. *Annu. Rev. Phys. Chem.* **1998**, *49*, 441-80

(9) Enderlein J.; Ambrose, W. P.; Goodwin, P. M.; Keller, R. A. In *Microsystem technology: A powerful tool for biomolecular studies*; Kohler, M.; Mejevaia, H. P.; Saluz, H. P., Eds; Birkhauser, Basel, **1999**, pp 311-29

(10) Moerner, W. E.; Orrit, M. *Science* **1999**, *283*, 1670-1676

(11) Weiss, S. *Science* **1999**, *283*, 1676-83

(12) Gimzewski, J. K.; Joachim, C. *Science* **1999**, *283*, 1683-1688

(13) Ishii, Y.; Yanagida, T. *Single Mol.* **2000**, *1*, 5-14

(14) Zander, C. *Fresenius J. Anal. Chem.* **2000**, *366*, 745-51

(15) Zander, C.; Enderlein J.; Keller, R. A., Eds; *Single Molecule Detection in Solution*, Wiley-VCH, Berlin, Germany, **2002**

(16) Moerner, W. E.; Fromm, D. P. *Rev. Sci. Instrum.* **2003**, *74*, 3597-3619

(17) Yeung, E. S. *Annu. Rev. Phys. Chem.* **2004**, *55*, 97-126

(18) Itano, W. M.; Bergquist, J. C.; Wineland, D. J. *Science* **1987**, *237*, 612

(19) Diedrich, F.; Krause, J.; Rempe, G.; Scully, M. O.; Walther, H. *IEEE J. Quantum Electron.* **1988**, *24*, 1314

(20) Dehmelt, H.; Paul, W.; Ramsey, N. F. *Rev. Mod. Phys.* **1990**, *2*, 525

(21) Binnig, G.; Rohrer, H. *Rev. Mod. Phys.* **1987**, *59*, 615–25

(22) Binnig, G.; Quate, C.F.; Gerber, C. *Phys. Rev. Lett.* **1986**, *56*, 930–33

(23) Hansma, P.K.; Elings, V.B.; Marti, O.; Bracker, C.E. *Science* **1988**, *242*, 209–16

(24) Radmacher, M.; Tillmann, R. W.; Fritz, M.; Gaub, H.E. *Science* **1992,** *257,* 1900–5

(25) Sakmann, B.; Neher, E. *Single Channel Recording*, Plenum, New York, **1995**

(26) Block, S. M. *Cell* **1998**, *93*, 5

(27) Mehta, A. D.; Reif, M.; Spudich, J. A.; Smith, D. A.; Simmons, R. M. *Science* **1999**, *283*, 1689

(28) Barnes, M. D.; Whitten, W. B.; Ramsay, J. M. *Anal. Chem.* **1995**, *67*, A418–23

(29) Bertie, J. E.; Vo-Dinh, T. *Appl. Spectrosc.* **1996**, *50*, A12–A20

(30) Moerner, W. E. *Science* **1994**, *265*, 46–53

(31) Xie, X. S.; Bian, R. X.; Dunn, R. C.; Wu, J. L.; Chen, P. C. **1996** *Near-field microscopy and spectroscopy of single molecules, single proteins, and biological membranes* In *Focus of Modern Microscopy*, River Edge, NJ: World Science

(32) Ishijima, A.; Yanagida, T. *Tends Biochem. Sci.* **2001**, *26*, 438-444

(33) Hirschfeld, T. *Appl. Opt.* **1976**, *15*, 2965–66

(34) Vale RD, Funatsu T, Pierce DW, Romberg L, Harada Y, Yanagida T. 1996. *Nature* 380:451–53

(35) Funatsu, T.; Harada, Y.; Tokunaga, M.; Saito, K.; Yanagida, T. *Nature* **1995**, *374*, 555-559

(36) Dickson, R. M.; Norris, D. J.; Tzeng, Y.-L.; Moerner, W. E. *Science* **1996**, *274*, 966-969

(37) Katz, E. D., Ed., *High Performance Liquid Chromatography: Principles and Methods in Biotechnology*, J. Wiley & Sons, Chichester, New York, , **1996**

(38) Fodor, S. P. A.; Rava, R. P.; Huang, X. C.; Pease, A. C.; Holmes, C. P.; Adams, C. P. *Nature*, 1993, *364*, 555

(39) Wooley, A. T.; Mathies, R. A. *Proc. Natl. Acad. Sci. U.S.A.* **1994**, *91*, 11348

(40) Tabata, H.; Cai, L. T.; Gu, J.-H.; Tanaka, S.; Otsuka, Y.; Sacho, Y.; Taniguchi, M.; Kawai, T. *Synthetic Metals*, **2003**, *133-134*, 469-472

(41) Lyubchenko, Y. L.; Shylakhtenko, L.S. *Proc. Natl. Acad. Sci. U.S.A.* **1997**, *94*, 496-501

(42) Herrick, J.; Benismon, A. *Chromosome Res.* **1999**, *7*, 409-423

(43) Herrick, J.; Michalet, X.; Konti, C.; Schurra, C.; Bensimon, A.; *Proc. Natl. Acad. Sci. U.S.A.* **2000**, *97*, 222-227

(44) Hill, E. K.; de Mello, A. J. *Analyst* **2000**, *125*, 1033-1036

(45) Shivashankar, G. V.; Libchaber, A. *Curr. Sci.* **1999**, *76*, 813-818

(46) Turner, S. W. P.; Levene, M.; Korlach, J.; Webb, W. W.; Craighead, H. G. *Proceedings of the Micro Total Analysis System*, Monterey, CA, 2001; pp 259-261

(47) Yoshinobu, B. *Proceedings of the Micro Total Analysis System*, Enschede, The Netherlands, 2000; pp 467-472

(48) Chan, V.; McKenzie, S. E.; Surrey, S.; Fortina, P.; Graves, D. J. *J. Colloid Interface Sci.* **1998**, *203*, 197-207

(49) Chan, V.; Graves, D. J.; Fortina, P.; McKenzie, S. E. *Langmuir* **1997**, *13*, 320-329

(50) Jordan, C. E.; Frutos, A. G.; Thiel, A. J.; Corn, R. M. *Anal. Chem.* **1997**, *69*, 4939-4947

(51) Bensimon, A.; Simon, A.; Chiffaudel, A.; Croquette, V.; Heslot, F.; Bensimon, D. *Science* **1994**, *165*, 2096-2098

(52) Bensimon, D.; Simon, A. J.; Croquette, V.; Bensimon, A. *Phys. Rev. Lett.* **1995**, *74*, 4754-4757

(53) Xue, Q.; Yeung, E. S. *Nature* **1995**, *373*, 681-683

(54) Houseal, T. W.; Bustamante, C.; Stump, R. F.; Maestre, M. F. *Biophys. J.* **1989**, *56*, 507-516

(55) Auzanneau, I.; Barreau, C.; Salome, L. C. R. *Acad. Sci., Ser. III* **1993**, *316*, 459-462

(56) Strick, T. R.; Allemand, J.-F.; Bensimon, D.; Croquette, V. *Biophys. J* **1998**, 74, 2016-2028

(57) Fan, F.-R. F.; Bard, A. J. *Science* **1995**, *267*, 871-874

(58) Chiu, D. T.; Zare, R. N. *J. Am. Chem. Soc.* **1996**, *118*, 6512-6513

(59) Nie, S.; Chiu, D. T.; Zare, R. N. *Science* **1994**, *266*, 1018-1021

(60) Yokota, H.; Saito, K.; Yanagida, T. *Phys. Rev. Lett.* **1998**, *80*, 4606-4609

(61) Enderlein, J. *Biophys. J* **2000**, *78*, 2151-2158

(62) Xu, X.; Yeung, E. S. *Science* **1997**, *276*, 1106-1109

(63) Ma, Y.; Shortreed, M. R.; Yeung, E. S. *Anal. Chem.* **2000**, *72*, 4640-4645

(64) Xu, X.; Yeung, E. S. *Science* **1998**, *281*, 1650-1653

(65) Shortreed, M. R.; Li, H.; Huang, W.-H.; Yeung, E. S. *Anal. Chem.* **2000**, *72*, 2879-2885

(66) Smith, S. B.; Aldridge, P. K.; Callis, J. B. *Science* **1989**, *243*, 203-206

(67) Ueda, M. *J. Biochem. Biophys. Methods* **1999**, *41*, 153-165

(68) Kang, S. H.; Shortreed, M. R.; Yeung, E. S. *Anal. Chem.* **2001**, *73*, 1091-1099

(69) Zheng, J.; Yeung, E. S. *Anal. Chem.* **2002**, *74*, 4536-4547

(70) Kang, S. H.; Yeung, E. S. *Anal. Chem.* **2002**, *74*, 6334-6339

(71) Zheng, J.; Li, H.-W.; Yeung, E. S. *J. Phys. Chem. B.* **2004**, *108*, 10357-10362

(72) Li, H-W.; Park, H-Y.; Porter, M. D.; Yeung, E. S. *Anal. Chem.* **2005**, 77, 3256-3260

(73) Lukacs, K. D.; Jorgenson, J. W. *J. High Resolut. Chromatogr.* **1985**, *8*, 407–11

(74) Lambert, W. J.; Middleton, D. L. *Anal.Chem.* **1990**, *62*, 1585–87

(75) Chen, C.-M. *Physica A* **2005**, *350*, 95–107

(76) Stein, V. M.; Bond, J. P.; Capp, M. W.; Anderson, C. F.; Record, M. T. Jr. *Biophys J* **1995**, *68*, 1063

ACKNOWLEDGEMENTS

I want to thank Dr. Yeung for the chance to work in his research group and his support during past few years. In his group I learned lessons that will last for my lifetime. I would also like to thank my committee members, Dr. Thiel and Dr. Miller for their understanding, help and support.

I thank Yeung group members for help, valuable discussions, support, and good time spent together. Especially, I want to thank Hung-Wing Li for her generous help with experiments and useful discussions.

Also, I want to thank Dr. Gail Christie (Department of Microbiology and Immunology, Virginia Commonwealth University) for providing us with PSP3 phage DNA and Nikola Pekas for all help in channel chip fabrication.

My family deserves special thanks for endless love, encouragement, and help that made all this possible.

This work was performed at Ames Laboratory under Contract No. W-7405-Eng-82 with the U.S. Department of Energy. The United States government has assigned the DOE Report number IS-T 2278 to this thesis. This work was supported by the Director of Science, Office of Basic Energy Sciences, Division of Chemical Sciences.